How acoustic waves are guided in buried subsurface channels in unconsolidated granular media

Vitalyi Gusev[1,*] and Vincent Tournat[2]
[1]*Laboratoire de Physique de l'Etat Condensé UMR-CNRS 6087, Université du Maine, Avenue Olivier Messiaen, 72085 Le Mans Cedex 9, France*
[2]*LAUM, CNRS, Université du Maine, Avenue Olivier Messiaen, 72085 Le Mans Cedex 9, France*
(Received 1 April 2008; published 3 September 2008)

We show the existence of natural subsurface channels that guide acoustic waves for periodic arrays of spherical grains under the influence of gravity. Downward propagation of acoustic rays can be stopped altogether as a result of a caustic whose origin lies in the continuous bending of rays as a result of a gravitationally induced increase of rigidity with depth. Upward propagation of acoustic rays, on the other hand, is attenuated by Bragg reflection arising from the continuous diminishing of rigidity in the direction of the surface, resulting in a vertical propagation constant that approaches a limited allowed value. Waves with different frequencies are shown to travel at different depths below the surface. The key conditions for the manifestation of the predicted wave modes are microscopic periodicity and macroscopic inhomogeneity of the medium.

DOI: 10.1103/PhysRevE.78.036602 PACS number(s): 43.20.+g, 46.40.Cd, 45.05.+x

INTRODUCTION

The phenomenon of wave guiding arises from multiple reflections of a field at an interface or as a consequence of spatially inhomogeneous material properties resulting in directional wave propagation. The simplest qualitative illustration of wave guiding from multiple reflection is shown in Fig. 1(a), where the propagation of a field along the x direction in a layer of a macroscopically homogeneous and microscopically continuous material is controlled by the reflection of the plane waves at two horizontal interfaces located at $y=y_s=0$ and $y=y_b$. We denote this configuration as a "surface-bottom" (s/b) configuration. In a macroscopically homogenous and microscopically continuous media the two-dimensional wave dispersion relation acquires the simple form

$$\omega^2 = c^2(k_x^2 + k_y^2), \tag{1}$$

where k_x and k_y are wave numbers for the x and y directions, c is the sound speed, and ω is the frequency. The term "microscopically continuous medium" is used here for a hypothetical medium where any possible structuring of a medium (even at atomic level) is neglected. Consequently the modification of wave dispersion relations due to real atomistic structure of the materials, for example acoustic anisotropy of the crystals, is neglected in Eq. (1). For a constant wave velocity c in the layer between y_s and y_b, the direction of the ray, defined by the slope k_x/k_y, does not change inside the slab for a fixed horizontal propagation constant k_x. Their direction changes abruptly at the interfaces in accordance with the Snell's law. In the case of total internal reflections the guided modes are not attenuated. In the case of vertical inhomogeneity of the physical properties of the slab, the wave speed becomes depth dependent, that is, $c=c(y)$, so that the vertical propagation constant k_y becomes depth dependent, $k_y=\sqrt{[\omega/c(y)]^2-k_x^2}$, and the direction of ray propagation changes continuously across the width of the slab, which is described as a bending or refraction of the rays [1]. If at some depth $y=y_c$ the condition $\omega/c(y_c)=k_x$, defining the position of a so-called caustic [1], is satisfied, then it follows that $k_y(y=y_c)=0$, the rays become horizontal, and, in the case of $c(y)$ continuously increasing with depth, the waves cannot propagate deeper into the medium. The rays are incident at the level $y=y_c$ at zero angle and change downward propagation for upward propagation. It follows that the field in the region $y>y_c$ becomes evanescent. Consequently a caustic, as a natural wave-guiding surface, can replace in Fig. 1(b) the lower wave-guiding interface at y_b. Such wave guiding can

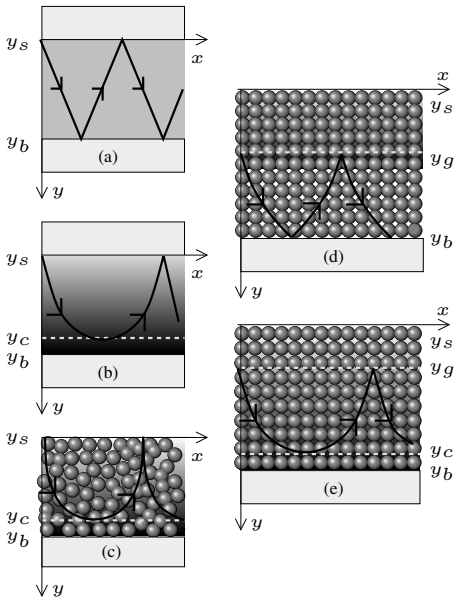

FIG. 1. Various physical realizations of a horizontal wave guide. (a) An homogeneous surface-bottom wave guide. (b) Wave guiding between a surface and a caustic. (c) Acoustic channeling between mechanically free surface of unconsolidated disordered granular medium and a caustic. (d), (e) Wave guiding in a microscopically periodic and macroscopically inhomogeneous media. (d) Gap-bottom undersurface wave guiding. (e) Gap-caustic under-surface wave guiding.

*Vitali.Goussev@univ-lemans.fr

be referred to as "surface-caustic" (s/c) wave guiding. Natural surface-caustic wave guiding is known, for example, for acoustic waves near the interface of water with marine sediments [2,3] and near the interface of sand (an example of an unconsolidated granular medium) with air [4–8] as shown in Fig. 1(c). For the typical sublinear power-law increase of material rigidity with depth the rays are incident on the surface vertically [7,8]. Note that in the case of nonmonotonous variation of the wave velocity along the y axis, caustics can stop both downward and upward propagation of waves as is known in the case of deep sound channels in the ocean [9].

Here we hypothesize that another mechanism, different from caustic natural wave guiding, can replace the upper wave-guiding interface in macroscopically inhomogeneous materials exhibiting microscopic periodicity. Our idea is based on the thesis that if the medium properties vary on a microscopic scale with a period D along the y direction, then there exists a maximum allowed value of the wave number $k_y^{\max}=\pi/D$ for the vertical propagation constant. The waves with larger k_y are evanescent due to effective multiple scattering. The phenomenon of limitation of vertical propagation constants is well documented for x-ray and Bragg diffraction in crystals, optical waves in photonic crystals [10], acoustic waves in layered structures [1], and phononic crystals [11]. For macroscopically inhomogeneous, microscopically periodic media, from the existence of $k_y^{\max}$, which implies a maximum allowed frequency $\omega_{\max}$, it follows that there must be a low-frequency boundary for the gap of frequencies forbidden for wave propagation. In accordance with the dispersion relation (1), the propagation of a ray in the direction of diminishing wave velocity is accompanied by an increase of the propagation constant k_y. If at some depth $y=y_g$, called in the following the "gap surface" or simply the "gap," the condition $k_y(y=y_g)=k_y^{\max}$ is satisfied and the vertical propagation constant approaches the limited allowed value, then at this level the wave will be Bragg reflected. In the case where $c(y)$ monotonously diminishes in the direction toward the surface, waves in the region $y<y_g$ are evanescent. We denote two new predicted configurations presented in Figs. 1(d) and 1(e) as "gap-bottom" (g/b) and "gap-caustic" (g/c) wave guiding, respectively. It is important that both channels $y_g<y<y_b$ and $y_g<y<y_c$ are "underground" in the sense that, if the gap position at $y=y_g$ is sufficiently separated from medium surface at $y=y_s$, then the evanescent field does not reach the surface, i.e., the waves cannot tunnel to the surface [11]. Hence they become "invisible" from the surface.

Although our hypothesis is straightforward, the arguments above cannot be considered as rigorous because the assumed periodicity at the microscopic level is necessarily accompanied by anisotropy in the properties of the medium and the wave velocity dispersion. Neither of these effects are accounted for in Eq. (1). In the following, we develop an analytical theory of the gap-bottom and gap-caustic channels for a particular case of acoustic waves in unconsolidated three-dimensional (3D) arrays of spherical elastic grains under gravity. Gravity induces a stress inside the packing of spheres dependent on the distance from the mechanically free, upper surface at $y=y_s$, which, as a result of the strong dependence of the rigidity of the Hertz-Mindlin contacts [12,13] between the spheres on stress, causes a depth-dependent sound velocity. The weak dependence of density on depth can be neglected. The medium under consideration is microscopically periodic with a spatial period of the order of the grain diameter D (leading to wave velocity dispersion) and macroscopically inhomogeneous along the direction of the gravity field. In addition it is elastically anisotropic consisting of a discrete ordered system of spheres. We incorporate both anisotropy and dispersion of wave velocity, reflecting microstructural features of the system, into a continuous description of wave guiding and prove the existence of gap-bottom and gap-caustic wave-guide acoustic modes by deriving their dispersion relations and determining the spatial boundaries of the underground channels.

It is of note that wave-guiding phenomena in media with periodically varying properties have recently attracted the interest of acousticians [14–16]. Much of the work in this field considers a wave-guiding surface at the interface between a continuous media and a macroscopically homogeneous crystal, resulting in an elastic-wave band-gap material. In terms of Fig. 1(a), such a model reduces to replacing the media in the regions $y<y_s$ and/or $y>y_b$ by a band-gap material. There has also been interest in the theory of surface acoustic waves where the discrete nature and internal periodicity of the crystals is taken into account, leading to wave dispersion and band gaps (see Ref. [17], and references therein). However, such work has focused only on macroscopically homogeneous media. Here we hypothesize that gap surfaces can exist in the band-gap material itself due to the natural influence of gravity, and that these surfaces in combination with other wave-guiding surfaces create natural channels for horizontal wave propagation.

THEORY

We hypothesize wave-guiding phenomenon in periodic three dimensional packing of spheres, which is a paradigmatic example for demonstrating the dependences of acoustic wave velocities on external loading in sediments [18–20]. We chose for analysis a simple cubic (sc) lattice of spheres [21–23], which permits understanding of the most important anisotropy-related features of the phenomenon, but which requires much less lengthy algebra than the analysis of face centred cubic [19,20] and hexagonal close [18] packing. Two different orientations of the packing relative to the gravity field are analyzed. The first configuration with the (0,1,0) axis of the granular lattice parallel to the gravitational acceleration $\vec{g}$ is presented in Fig. 2(a). The second configuration where the (1,1,0) axis of the granular lattice is parallel to $\vec{g}$, as shown in Fig. 2(b), is obtained by 45° rotation of the first around the z axis. We denote these configuration as $\oplus$ and $\otimes$ configurations, respectively. To demonstrate the physical principles of the wave-guiding phenomenon we analyze, neglecting rotations of the beads, the propagation of shear waves polarized along the z axis with the wave vector $\vec{k}$ lying in the (x, y) plane, i.e., $k_z=0$. We study wave process in macroscopically inhomogeneous medium in the framework of geometrical acoustics [the Wentzel-Kramers-Brillouin (WKB)] approximation [1,24], which is valid under the condition that relative changes of the acoustic wave number on

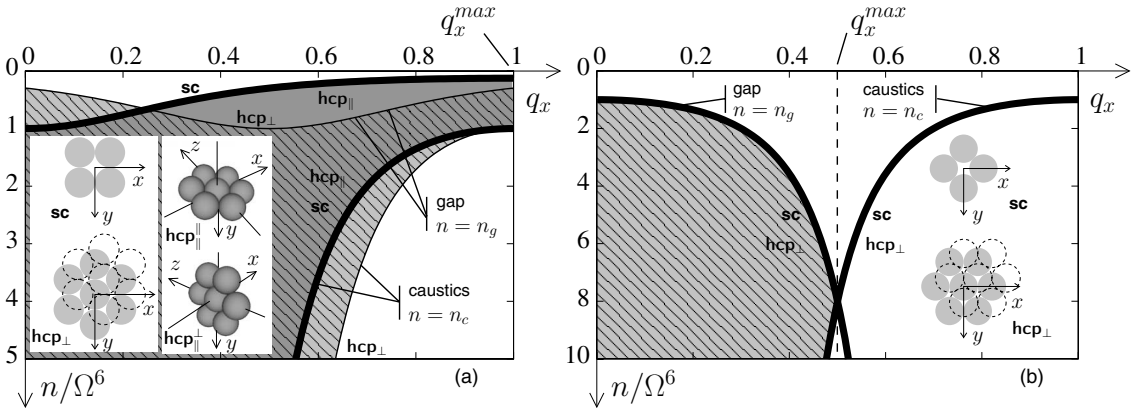

FIG. 2. Wave guiding of bulk acoustic waves between a gap surface and a caustic in an inhomogeneous granular crystal. The unconsolidated packings of Hertz-Mindlin elastic spheres of different symmetries and orientations relative to the gravity field are presented in the insets. The in-depth positions of the wave-guiding surfaces are plotted as the functions of the dimensionless frequency Ω and the dimensionless wave number q_x of the bulk acoustic waves. Integer number n ($n \geqslant 0$) counts the layers of periodic granular medium starting from its surface. The surface of Bragg reflection or the gap surface is located at a depth $n=n_g$ and the caustic surface is located at a depth $n=n_c$.

the scale of the acoustic wavelength are small, i.e., $|\vec{\nabla}k|/k^2 \ll 1$. In the array of spheres, the acoustic wavelength can be of the order of the sphere diameter D; consequently, ray theory should be valid only if the material properties vary slowly on the length scale of D. The wave dispersion relation in ray theory is derived for a macroscopically homogeneous material but with the parameters of the dispersion relation allowed to vary slowly with coordinate [1].

The equation of motion for the horizontal column of spheres centered at $x=Dm$, $y=Dn$, where m and n are integers, in the $\oplus$ configuration is $M\partial^2 u_{m,n}/\partial t^2 = \eta(u_{m,n+1} + u_{m,n-1} + u_{m+1,n} + u_{m-1,n} - 4u_{m,n})$, where M is the mass of the sphere, $u_{m,n}$ is its displacement along the z axis, and η is the shear rigidity of the contact. The solution of these equations in the form $u_{m,n} \propto \exp(i\omega t - ik_x Dm - ik_y Dn)$ leads to the anisotropic dispersion relation

$$(\omega/\omega_{\max})^2 = \sin^2(Dk_x/2) + \sin^2(Dk_y/2), \tag{2}$$

which predicts that, due to the microscopic periodicity of the medium, there is dispersion in the wave velocity. The allowed propagation constants are restricted by $k_x^{\max} = k_y^{\max} = \pi/D$, and there exists a forbidden domain of high frequencies for all the directions of bulk wave propagation. In Eq. (2) $\omega_{\max} \equiv 2\sqrt{\eta/M}$ denotes the maximum frequency allowed for bulk shear wave propagation along the surface, i.e., when $k_y=0$.

A granular medium is modelled above as a packing of perfectly rigid spheres connected by springs. This is a well-confirmed model for a packing of elastic beads in contact in the case where due to weak loading the diameter d of the contact between the spheres is much smaller than the diameter D of the beads ($d \ll D$). In this situation the Hertz-Mindlin theory of contacts [13] predicts that a small volume of a bead near the contact (of a characteristic dimension d of the order of the contact diameter) plays the role of a soft spring, while the rest of the bead can be considered as being perfectly rigid. The effective rigidity of the spring is controlled not just by the shear modulus μ of the material composing the beads but also by the diameter of the contact $\eta \propto \mu d$ and is small under weak loading. As a consequence the acoustic waves are propagating in the weakly loaded granular medium much slower than inside the individual beads. This slow motion could be qualitatively viewed as a slow transfer of vibrations from one bead to another because of weak coupling between the beads and multiple scattering of fast acoustic waves inside the beads resulting in the motion of the beads as nearly rigid masses. The characteristic resonance frequency of vibration of a rigid bead near its equilibrium position in the packing can be estimated as $\omega_{\max} \propto \sqrt{\eta/M} \propto \sqrt{\mu d/(\rho D^3)}$, where ρ denotes the density of the beads. This is also an estimate for the maximum frequency of the propagating acoustic waves for the model of rigid spheres connected by the springs. Characteristic resonance frequency of internal vibration of an individual elastic bead (due to its elasticity) can be estimated as an inverse of a time for acoustic wave propagation across the bead $\omega_{\text{res}} \propto \sqrt{\mu/\rho}/D \propto \sqrt{\mu/(\rho D^2)}$. Consequently $\omega_{\max}/\omega_{\text{res}} \propto \sqrt{d/D}$ and under the condition $\sqrt{d/D} \ll 1$ there is a clear separation of the frequency scales. At frequencies lower than ω_{res} the phenomenon of slow wave propagation including the band-gap effect, taking place around $\omega_{\max}$, can be described by the model of rigid masses connected by the springs. Note that in this model the absorption of acoustic waves in the material composing the grains and also absorption due to possible interaction of grains with air, saturating the pores of the packing, is completely neglected in order to concentrate attention on the effects related to microscopic periodicity of inhomogeneous medium.

The predictions based on Eq. (2) are not modified qualitatively if rotations of the spheres are included in the analysis. The existence of the additional allowed frequency band for the rotational waves, similar to the ensemble of optical phonons in crystals, separated by a gap from the frequency band of shear waves [22,23,25,26] is not essential for the purposes of our analysis.

The dispersion relation for the $\otimes$ configuration can be derived from Eq. (2) by rotation of the coordinate system. If, in both configurations, the propagation constants are normalized to the maximum allowed value along the x direction $k_{x,y}/k_x^{\max} \equiv q_{x,y}$, and the frequency is normalized to its band edge value $\omega_{\max}(n)$ for bulk waves traveling in the x direction $\omega/\omega_{\max}(n) \equiv \Omega(\omega,n)$, the dispersion relations for $\oplus$ and $\otimes$ configurations take the form

$$\Omega^2(\omega,n^{\oplus/\otimes}) = \sin^2(\pi q_x/2) + \sin^2(\pi q_y/2) - (1 \mp 1)\sin^2(\pi q_x/2)\sin^2(\pi q_y/2), \quad (3)$$

where the index n, which numbers the layers of the array along the vertical coordinate, accounts for the macroscopic inhomogeneity of the medium in the gravity field. It should not be forgotten that the distance between successive horizontal, and vertical, layers of spheres is different in the two configurations considered here (see Fig. 2), leading to different values of $k_x^{\max}$ and $\omega_{\max}(n)$. In the accepted normalization, the position of the caustic $n=n_c$ defined from the condition $q_y=0$ is the same in both configurations

$$\Omega^2(\omega,n_c^{\oplus/\otimes}) = \sin^2(\pi q_x/2), \quad n_c^{\oplus/\otimes} = \Omega^{-1}[\omega,\sin(\pi q_x/2)]. \quad (4)$$

The anisotropy influences $n_c^{\oplus/\otimes}$ in Eq. (4) implicitly through the dispersion relation of the wave-guide mode $\omega=\omega(k_x)$, which is different in the two configurations. The positions of the gaps, $n=n_g$, defined from the condition $q_y=1$, are different in the two configurations

$$\Omega^2(\omega,n_g^{\oplus/\otimes}) = 1 \pm \sin^2(\pi q_x/2), \quad n_g^{\oplus/\otimes} = \Omega^{-1}[\omega,\sqrt{1 \pm \sin^2(\pi q_x/2)}]. \quad (5)$$

They are influenced by the anisotropy, which controls the deviation of $n_g^{\oplus/\otimes}$ from the horizontal level in Fig. 2, explicitly. Assuming that natural loading by gravity induces monotonously increasing $\omega_{\max}(n)$ and monotonously decreasing $\Omega(\omega,n)$, we arrive from comparison of Eqs. (4) and (5) at the following conclusions. In the $\oplus$ configuration $n_c > n_g$ and the gap-caustic wave guiding is potentially possible for all allowed horizontal propagation constants $0 \leqslant q_x \leqslant 1$ [see Fig. 2(a)]. In the $\otimes$ configuration, gap-caustic wave guiding is potentially possible only in a bandwidth of half this width $0 \leqslant q_x \leqslant 1/2$ [see Fig. 2(b)]. For larger propagation constants, the gap is below the caustic $n_c < n_g$. The striking difference between two configurations is the consequence of anisotropy alone. In the $\oplus$ configuration the maximum spatial period, the smallest $k^{\max}$, and the lowest $\omega_{\max}$ for the bulk modes are all along the surface. For rays propagating at an angle to the surface, the gap edge $\omega_{\max}$ is not lower, so that wave-guide modes even with $q_x=1$ are allowed. In the $\otimes$ configuration, the minimum spatial period, the largest $k^{\max}$, and the highest gap edge $\omega_{\max}$ for the bulk modes are all along the surface. For rays propagating at an angle to the surface, the allowed spectral interval $0 \leqslant \omega \leqslant \omega_{\max}$ is narrower. Thus, for example, rays with $q_x=1$ and any $q_y \neq 0$ cannot propagate, they are purely evanescent. In the propagating gap-caustic wave-guide mode, the vertical propagation constant should continuously change from $q_y=0$ at the caustic to $q_y=1$ at the gap. It follows that the interval $0 \leqslant q_x \leqslant q_x^{\max}$ for the existence of gap-caustic wave guiding is determined by the condition that even for $q_x=q_x^{\max}$, all values of q_y in the range $0 \leqslant q_y \leqslant 1$ should be allowed. In the $\otimes$ configuration, this results in $q_x^{\max}=1/2$ [Fig. 2(b)]. Thus as a consequence of the packing anisotropy the domain $0 \leqslant q_x \leqslant q_x^{\max}$ of a possible existence of wave-guiding phenomena (for which the caustic should be deeper than the gap: $n_c > n_g$, the shaded and/or grey regions in Fig. 2) is different in two configurations.

Using a more lengthy algebra we have derived the dispersion relations for the propagation of plane shear acoustic phonons in hexagonal close packing (hcp) of frictionless beads. The dispersion relations for the waves polarized perpendicular ($\mathrm{hcp}_\perp$) to the planes with hexagonal arrangement of the beads [in the coordinate system presented in inset $\mathrm{hcp}_\perp$ in Fig. 2(b)] are $M\omega^2 = 4\eta\{1 \pm \sqrt{1+4\cos(k_x D/2)[\cos(k_x D/2)+\cos(k_y\sqrt{3}D/2)]}/3\}$. These relations describe both optical phonons branch and acoustical phonons branch. The latter is specified by the condition $\omega(k_x=0,k_y=0)=0$ and is the subject of our analysis here. The dispersion relations for the acoustical phonons polarized parallel ($\mathrm{hcp}_\parallel$) to the planes with hexagonal arrangement of the beads [parallel to z axis in insets $\mathrm{hcp}_\parallel^\parallel$ and $\mathrm{hcp}_\parallel^\perp$ in Fig. 2(a)] for the case $\mathrm{hcp}_\parallel^\parallel$, where the hexagon is parallel to the surface of the packing, are $M\omega^2 = 2\eta[\sin^2(k_x\sqrt{3}D/4)+\sin^2(k_y D/\sqrt{6})]$. Here η denotes the normal rigidity of a Hertzian contact. The dispersion relations for two other configurations presented by insets $\mathrm{hcp}_\perp$ and $\mathrm{hcp}_\parallel^\perp$ in Fig. 2(a) can be obtained from those given above by the transformation of the coordinate system. In Figs. 2(a) and 2(b), after the normalizations performed similarly to the sc case, we present the positions of the gaps and the caustics for the orientations $\mathrm{hcp}_\perp$ and $\mathrm{hcp}_\parallel$ of the hexagonal plane in space. These results provide assurance that there is an allowed zone for channeling in the case of close packing and that the role of anisotropy in sc and hcp cases could be similar. Moreover, there is no qualitative difference between the dispersion relations for some particular hcp configurations, such as $\mathrm{hcp}_\parallel^\parallel$ or $\mathrm{hcp}_\parallel^\perp$ [Fig. 2(a)] and sc$\oplus$ dispersion relations in Eq. (2). In both $\mathrm{hcp}_\parallel$ configurations presented in Fig. 2(a) the domain of wave guiding coincides with that for the sc$\oplus$ configuration. Due to this the predictions derived below for the sc$\oplus$ case are valid for the $\mathrm{hcp}_\parallel$ case as well. The domains of existence of wave guiding phenomena in $\mathrm{hcp}_\perp$ configurations are shaded in Figs. 2(a) and 2(b). In the $\mathrm{hcp}_\perp$ configuration presented in Fig. 2(b) the domain of wave guiding coincides with that for the sc$\otimes$ configuration. To establish real spatial positions $n=n_c(q_x)$ and $n=n_g(q_x)$ for the boundaries of the wave guide the curves in the figure should be rescaled after finding the dispersion relation $\Omega=\Omega(q_x)$ for the guided acoustic modes (see Fig. 3).

In order to predict with the help of Eqs. (4) and (5) the position of the gap-caustic channel under the surface, the dispersion relation of the wave-guide modes $\omega=\omega(q_x)$ should be found. For deriving the dispersion relation we are using the geometrical acoustics approximation and the Bohr-Sommerfeld condition of constructive interference [27], also known in acoustics as the condition of transverse resonance [28]. The phase shift accumulated by a ray in its vertical propagation from the upper wave-guiding surface at $n=n_{\min}$ to the lower wave-guiding surface at $n=n_{\max}$ and back should be an integer number p of 2π

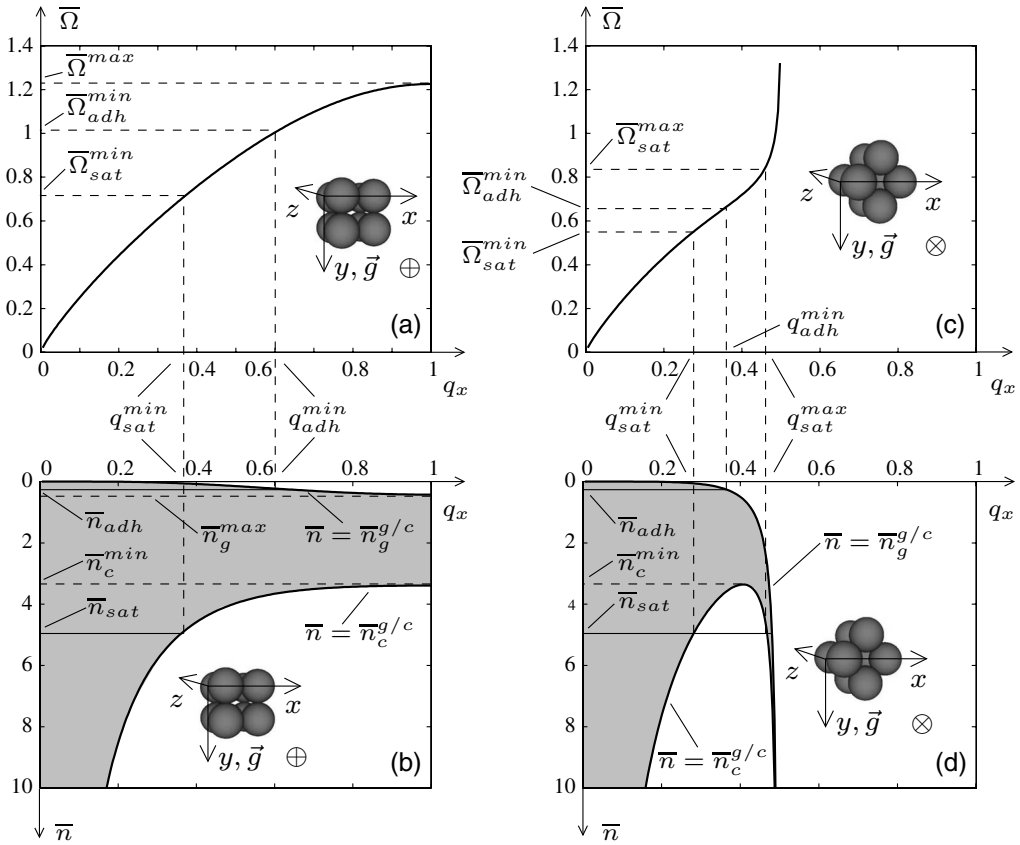

FIG. 3. Wave-guide acoustic modes channeling between a gap and a caustic in an inhomogeneous granular crystal. The dispersion relations $\bar{\Omega}=\bar{\Omega}(q_x)$ for the gap-caustic acoustic modes guided between the gap at depth $\bar{n}=\bar{n}_g^{g/c}$ and the caustic at depth $\bar{n}=\bar{n}_c^{g/c}$ are presented in (a) and (c) for $\oplus$ and $\otimes$ configurations, respectively. The corresponding under-surface channels are grey in (b) and (d).

$$\sum_{n_{\min}}^{n_{\max}} q_y \cong \int_{n_{\min}}^{n_{\max}} q_y dn = p, \quad p = 1,2,3,\ldots, \tag{6}$$

where the summation has been transformed into integration based on the geometrical acoustics approximation for a slow dependence of q_y on the discrete coordinate n, which, consequently, can be treated as a continuous one. However it is well-known that geometrical acoustics is not valid in the vicinity of caustics [1,24]. It can be also verified that the validity condition $(\partial k_y/\partial y)/k_y^2 \ll 1$ necessary for geometrical acoustics does not hold in the vicinity of the gap either. Nevertheless the condition in Eq. (6) becomes progressively more and more precise with increasing p when the additional constant (p-independent) phase losses accumulated in the domains of invalidity of the geometrical acoustics approximation become negligible in comparison with the total phase shift increasing proportionally p. That is why, in order to be sure of the validity of all the effects predicted below in the framework of ray acoustics, we will assume in the following $p \gg 1$ (although already $p \geqslant 3$ could be precise enough in practice [1,7,8]).

To proceed further in the analysis we accept Hertz-Mindlin model for the shear rigidity of the contacts between the spheres [12,13]. In this model the rigidity is the nonlinear power-law function of the normal force F acting on the contact (i.e., $\eta \propto F^{1/3}$), resulting in the following unified presentation of $\omega_{\max}(n)$ for both configurations $\omega_{\max}(n) = \omega_{\max}(1)n^{1/6}$, although $\omega_{\max}(1)$ is different in the $\oplus$ and $\otimes$ configurations $(\omega^{\oplus}_{\max}(1) = 2^{1/12}\omega^{\otimes}_{\max}(1) = 2[\frac{3(1-\nu)}{2-\nu}]^{1/2} \times [\frac{4E}{3(1-\nu^2)M}]^{1/3}(\frac{gD}{2})^{1/6}$, where ν is the Poisson's ratio and E is the Young modulus of the spheres). Introducing an n-independent dimensionless frequency $\Omega \equiv \omega/\omega_{\max}(1)$ we reduce the above derived general presentation in Eqs. (3)–(5) to a particular one for Hertz-Mindlin contacts under gravity

$$q_y^{\oplus/\otimes} = (2/\pi)\arcsin\sqrt{(\Omega^2 n^{-1/3} - s^2)/(1 \pm s^2 - s^2)} \equiv q_y^{\oplus/\otimes}(\Omega^2 n^{-1/3}/a_{\oplus/\otimes}, s^2/a_{\oplus/\otimes}), \tag{7}$$

$$n_c^{\oplus/\otimes} = (\Omega/s)^6, \quad n_g^{\oplus/\otimes} = [\Omega/\sqrt{1 \pm s^2}]^6, \tag{8}$$

where we have used the compact notations $s \equiv \sin(\pi q_x/2)$ and $a_{\oplus/\otimes} \equiv 1 \pm s^2 - s^2$. The domains of possible wave guiding described by Eq. (8) are presented in Fig. 2. However, it should be expected that, when the dispersion relation $\Omega = \Omega(q_x, p)$ is found, the shape of the wave-guiding domain on the plane (q_x, n) might be very different from what is given in Fig. 2 (see Fig. 3).

The integration in Eq. (6), when on substituting Eq. (7), can be carried out analytically. The dispersion relation for the modes guided between two levels in the depth of the gravity-loaded periodic packing of elastic spheres is

$$\int_{n_{\min}}^{n_{\max}} q_y(\Omega^2 n^{-1/3}/a_{\oplus/\otimes}, s^2/a_{\oplus/\otimes})dn = \Omega^6[I(\Omega^2 n_{\max}^{-1/3}/a_{\oplus/\otimes}) - I(\Omega^2 n_{\min}^{-1/3}/a_{\oplus/\otimes})] = p, \quad (9)$$

where

$$I(\sigma) = \frac{2}{\pi a^3}\left\{\frac{\arcsin\sqrt{\sigma - s^2/a}}{\sigma^3} - \frac{1}{8c^2}\left[\frac{3b\sigma + 2c}{\sigma^2}\sqrt{-\sigma^2 + b\sigma - c} + \frac{3b^2 - 4c}{2\sqrt{c}}\arctan\left(\frac{b\sigma - 2c}{2\sqrt{c}\sqrt{-\sigma^2 + b\sigma - c}}\right)\right]\right\},$$

$$a \equiv a_{\oplus/\otimes}, \quad b \equiv 1 + \frac{2s^2}{a}, \quad c \equiv \left(1 + \frac{s^2}{a}\right)\frac{s^2}{a}.$$

It should not be forgotten that the positions of the levels $n_{\min}$ and/or $n_{\max}$ could themselves be dependent on Ω and q_x as, for example, in the configurations with gaps and/or caustics. In these cases Eq. (9) together with Eq. (8) constitute a self-consistent problem of simultaneous determination of the p-mode dispersion relation and the boundaries of the channel where this mode propagates.

The dispersions relations for the gap/caustic mode of order p and the boundaries of the channel, evaluated with the help of Eq. (9) (where $n_{\min}=n_g$ and $n_{\max}=n_c$) and Eq. (8), are presented in Fig. 3. The theory predicts [see Figs. 3(b) and 3(d)] narrowing of the gap-caustic channel width with an increase in the wave propagation constant q_x. The frequency of the mode scales as $p^{1/6}$ and the depth of the channel localization as p with the order p of the wave-guide mode. The higher-order modes have higher frequencies and are guided deeper into the medium. As a consequence, in the scaled variables $\bar{\Omega} \equiv \Omega/p^{1/6}$ and $\bar{n} \equiv n/p$, the presentation in Fig. 3 is valid for modes of all possible orders. The dispersion relations for long wavelengths reduce in the limit $q_x \to 0$ in both configurations to $\Omega_{\oplus/\otimes} \approx (8p/3)^{1/6} q_x^{5/6}$ known for the wave-guide modes in the channel formed by the free surface and the caustics in disordered granular packing [7,8] [Fig. 1(c)]. The width of the channel scales as $n_c \propto (\Omega/q_x)^6 \propto q_x^{-1} \propto \Omega^{-6/5}$. Periodicity in the packing of spheres is not important for these modes, which have the wavelength significantly exceeding the diameter of the spheres.

In the $\oplus$ configuration the range of accessible frequencies is bounded as shown in Fig. 3(a). The maximum frequency of the p mode $\bar{\Omega}_{\max}$ is achieved for the maximum allowed horizontal propagation constant $q_x=1$ when the group velocity of the gap-caustic mode is equal to zero. Correspondingly there exist the deepest position of the gap surface $\bar{n}_g^{\max}$, the shallowest position of the caustics $\bar{n}_c^{\min}$, and the minimum channel width all realized at $q_x=1$ as can be seen in Fig. 3(b).

As Fig 3(c) shows, in the $\otimes$ configuration, the frequency of the g/c mode diverges $[\bar{\Omega} \propto (1/2 - q_x)^{-1/6}]$ accompanied by divergence of both phase and group velocities when $q_x \to 1/2$. In this limit both channel boundaries penetrate infinitely deep into the medium $\bar{n}_g \propto \bar{n}_c \propto (1/2 - q_x)^{-1} \to \infty$ but the channel width remains finite $\bar{n}_c - \bar{n}_g \to 2$. The closest to the surface position of the caustics $\bar{n}_c^{\min}$ is achieved at $q_x \approx 0.42$ [see Fig. 3(d)].

The prediction for the $\otimes$ configuration of modes with infinitely high frequencies is the consequence of the possibility of infinite medium rigidity assumed in the model $\omega_{\max}(n) = \omega_{\max}(1)n^{1/6}$. In reality, in granular packing, the growth of rigidity with depth will necessarily saturate as the rigidity of the granular packing cannot exceed the rigidity of individual grains. Figures 3(b) and 3(d) permit visualization of the influence of a maximum rigidity existence in the medium on the phenomenon of gap/caustic wave guiding. Let the rigidity growth described by Hertz-Mindlin theory saturate abruptly at a depth $n=n_{\text{sat}}$ [$\omega_{\max}(n) \propto n^{1/6}$ for $n \leqslant n_{\text{sat}}$, $\omega_{\max}(n) \propto n_{\text{sat}}^{1/6}$ for $n \geqslant n_{\text{sat}}$] marked in Figs. 3(b) and 3(d). Then all the parts of the caustic surface, which are below the horizontal level $\bar{n}_{\text{sat}}$, cannot be physically realized. The wave guiding will be possible only in the restricted interval of propagation constants q_x and only if $\bar{n}_{\text{sat}}$ exceeds $\bar{n}_c^{\min}$. In the $\oplus$ configuration for $\bar{n}_{\text{sat}} > \bar{n}_c^{\min}$ the gap/caustic channeling is allowed for $q_{\text{sat}}^{\min} \leqslant q_x \leqslant 1$, where $q_{\text{sat}}^{\min}$ is determined by the intersection point of the saturation level with caustic level in Fig. 3(b). Wave guiding in the frequency band $0 \leqslant \bar{\Omega} \leqslant \bar{\Omega}_{\text{sat}}^{\min}$ [see Fig. 3(a)] cannot take place. In the $\otimes$ configuration the saturation level for $\bar{n}_{\text{sat}} > \bar{n}_c^{\min}$ intersects the caustic level in two points $q_x = q_{\text{sat}}^{\min}$ and $q_x = q_{\text{sat}}^{\max} < 1/2$ and the gap-caustic wave guiding is allowed only for $q_{\text{sat}}^{\min} \leqslant q_x \leqslant q_{\text{sat}}^{\max} < 1/2$. Consequently as soon as the physical reality of saturation of the medium rigidity growth with depth is taken into account, the theory predicts a finite frequency band $\bar{\Omega}_{\text{sat}}^{\min} \leqslant \bar{\Omega} \leqslant \bar{\Omega}_{\text{sat}}^{\max}$ as shown in Fig. 3(c) for the existence of the gap-caustic guided acoustic modes. In summary if the growth of the granular medium rigidity with depth saturates at the level $\bar{n}=\bar{n}_{\text{sat}}$, exceeding the shallowest position of the caustic $\bar{n}_c^{\min}$ [see Figs. 3(b) and 3(d)], then the wave-guiding phenomena persist only for $q_{\text{sat}}^{\min} \leqslant q_x \leqslant 1$ ($\bar{\Omega}_{\text{sat}}^{\min} \leqslant \bar{\Omega} \leqslant \bar{\Omega}^{\max}$) in the $\oplus$ configuration [Figs. 3(a) and 3(b)] and only for $q_{\text{sat}}^{\min} \leqslant q_x \leqslant q_{\text{sat}}^{\max} \leqslant 1/2$ ($\bar{\Omega}_{\text{sat}}^{\min} \leqslant \bar{\Omega} \leqslant \bar{\Omega}_{\text{sat}}^{\max}$) in the $\otimes$ configuration [Figs. 3(c) and 3(d)]. The gap-caustic wave-guiding phenomenon completely disappears if $\bar{n}_{\text{sat}} > \bar{n}_c^{\min}$.

Figures 3(b) and 3(d) also describe the case of existence of a minimum positive medium rigidity, which could result from adhesion between the spheres or the formation of liquid bridges between the spheres in the presence of moisture [29,30] both providing in the medium an internal pressure unrelated to gravity. Let us assume that this additional pressure is numerically equal to the pressure created by gravity at a depth $n=n_{\text{adh}}$. Then, the influence of the increased adhesion can be associated with the downward motion of the horizontal level $\bar{n}=\bar{n}_{\text{adh}}$, corresponding in the modified coordinates $\bar{n} \to \bar{n}_{\text{adh}} + \bar{n}$ to mechanically free surface of the medium [7,8], as shown in Figs. 3(b) and 3(d). As long as $\bar{n}=\bar{n}_{\text{adh}}$ intersects the predicted level $\bar{n}=\bar{n}_g$ at some $q_x = q_{\text{adh}}^{\min}$, wave guiding between the gap and the caustics [Fig. 1(e)] in the region $0 \leqslant q_x \leqslant q_{\text{adh}}^{\min}$ is replaced by wave guiding between the mechanically free surface, which in the coordinate system of Figs. 3(b) and 3(d) is located at $\bar{n}=\bar{n}_{\text{adh}}$, and the caustic [7,8].

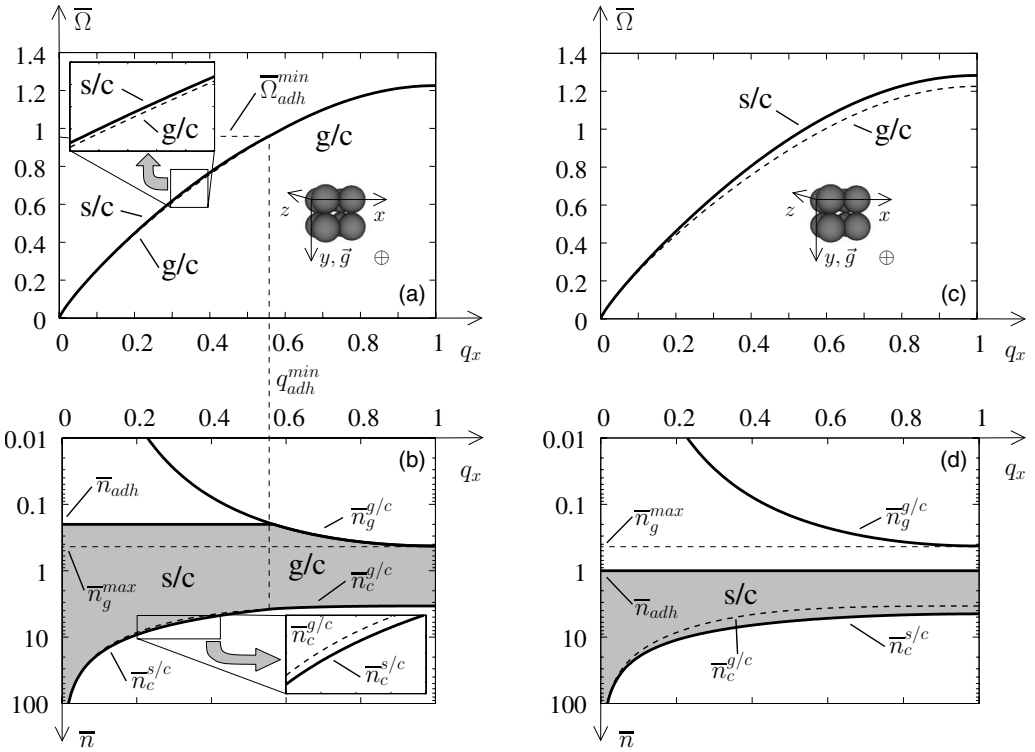

FIG. 4. Influence of adhesion between the grains on the wave-guiding phenomenon in granular crystals. The modification by adhesion of the dispersion relations $\bar{\Omega}=\bar{\Omega}(q_x)$ for the wave guide modes and the in-depth positions of the channel [grey in (b), (d)] in $\oplus$ configuration.

Adhesion introduces a low-frequency cutoff for gap-caustic channeling $\bar{\Omega} \geqslant \bar{\Omega}^{\min}_{\text{adh}}$ [see Figs. 3(a) and 3(c)]. To find a dispersion relation for the generalized mode guided between the caustic, and either the gap or the surface, the Ω roots of Eq. (9) should be found for $n_{\max}=n_c$ and $n_{\min}=\max[n_g, n_{\text{adh}}]$. In summary, if there exists adhesion between the grains, which creates an internal pressure equivalent to the gravity-induced pressure at some depth $\bar{n}=\bar{n}_{\text{adh}}$ in the packing without adhesion [see Figs. 3(b) and 3(d)], then for the wave numbers q_x, satisfying the condition $\bar{n}^{g/c}_g(q_x) < \bar{n}_{\text{adh}}$, the gap-caustic wave guiding in the domain $0 \leqslant q_x \leqslant q^{\min}_{\text{adh}}$ $(0 \leqslant \bar{\Omega} \leqslant \bar{\Omega}^{\min}_{\text{adh}})$ is replaced by surface-caustic wave guiding. The physics of this is clear. The existence of the minimum rigidity in the medium introduces the minimum value for $\omega_{\max}$. The frequencies lower than this threshold value cannot be stopped by the gap and they reach the mechanically free surface. In the $\oplus$ configuration the opportunity for g/c wave guiding completely disappears when $\bar{n}_{\text{adh}} > \bar{n}^{\max}_{\text{gap}}$.

For illustration, the dispersion relations and the boundaries of the channel for the $\oplus$ configuration are shown in Figs. 4(a) and 4(b) for the case $\bar{n}_{\text{adh}} < \bar{n}^{\max}_{\text{gap}}$, and in Figs. 4(c) and 4(d) for the case $\bar{n}_{\text{adh}} > \bar{n}^{\max}_{\text{gap}}$. In the case $\bar{n}_{\text{adh}} < \bar{n}^{\max}_{\text{gap}}$ [Figs. 4(a) and 4(b)] the gap as an upper boundary of the channel is replaced for $0 \leqslant q_x \leqslant q^{\min}_{\text{adh}}$ by the mechanically free surface located at $\bar{n}=\bar{n}_{\text{adh}}$ in Fig. 4(b). In the case $\bar{n}^{\max}_g \leqslant \bar{n}_{\text{adh}}$ [Figs. 4(c) and 4(d)] the gap-caustic wave guiding is completely replaced by surface-caustic wave guiding. These replacements lead to the modification of the dispersion relations for the wave-guide modes [compare continuous s/c and dashed g/c curves for surface/caustic and gap/caustic channeling in Figs. 4(a) and 4(c)] and also to the shift of the lower boundary of the channel, i.e., of the caustic [compare continuous $\bar{n}^{\text{s/c}}_c$ and dashed $\bar{n}^{\text{g/c}}_c$ curves in Figs. 4(b) and 4(d)].

More complicated phenomena could be expected when the granular medium is not semi-infinite, but just a layer of thickness n_b on a substrate. To avoid analysis of the substrate motion we assume it to be infinitely rigid. Then any motion at depths $\bar{n} \geqslant \bar{n}_b$ is forbidden. There is an obvious difference between the case of rigidity saturation at the depth $\bar{n}=\bar{n}_{\text{sat}}$ discussed above [see Figs. 3(b) and 3(d)] and the existence of the rigid bottom at the same level $\bar{n}=\bar{n}_b=\bar{n}_{\text{sat}}$. The saturation surface completely eliminates the possibility of gap-caustic channeling in domains where $\bar{n}^{\text{g/c}}_c > \bar{n}_b=\bar{n}_{\text{sat}}$, while the rigid bottom potentially replaces in the same domains gap-caustic wave guiding by gap-bottom wave guiding. The other important point is the possibility for existence of two modes of the same order p in the case where the lower boundary of the channel is fixed. The possibility for existence of two p modes, high-frequency (HF) mode and low-frequency (LF) mode, in a gap-bottom channel can be ascribed to the diminishing of the channel width with increasing frequency. This, in turn, is caused for the fixed lower boundary (bottom) of the channel by the penetration of the upper boundary (gap) deeper and deeper into the depth of the medium with increasing frequency, because, to stop upward propagation of high frequencies the forbidden band edge, $\omega_{\max}$ should be higher than one to stop low frequencies. This condition is achievable for larger rigidities, that is, at larger depths from the surface than for low frequencies. Simultaneously, the rays of high frequencies have larger vertical propagation constants q_y for a fixed horizontal propagation constant q_x than the rays of low frequencies and, correspondingly, the field oscillates faster along the vertical

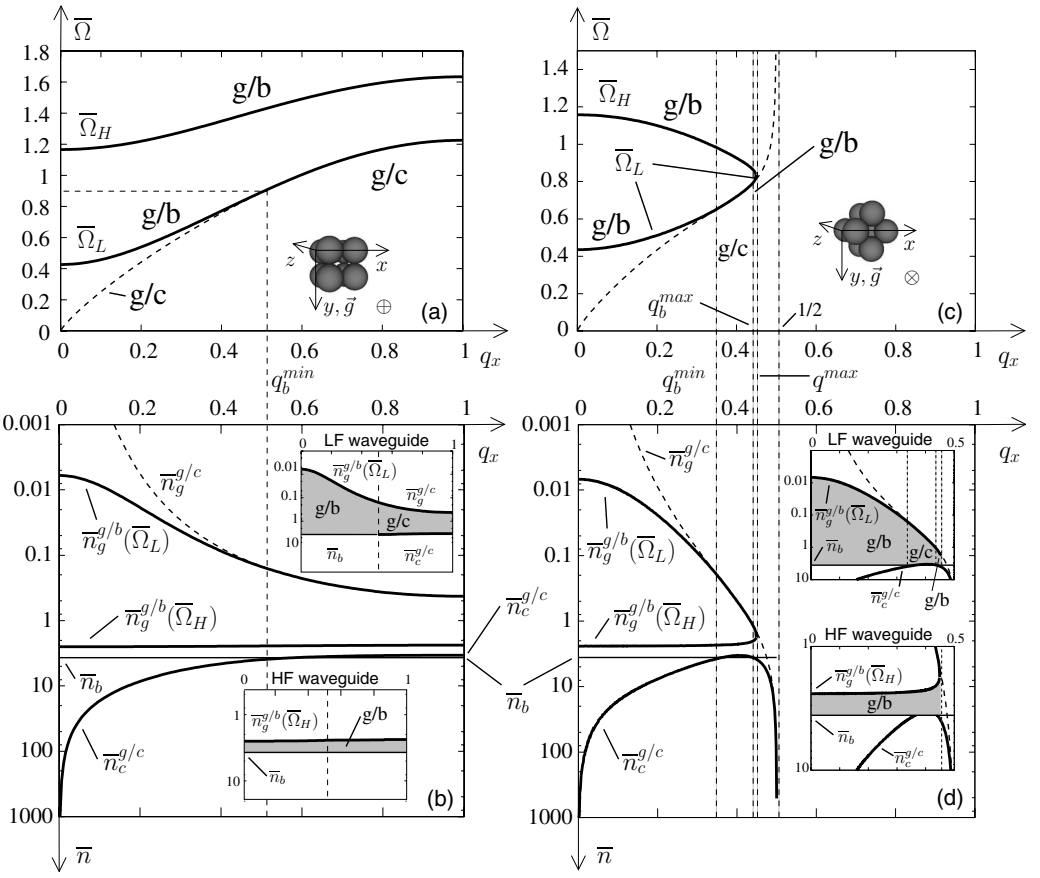

FIG. 5. Influence of a finite depth of granular medium on the wave-guiding phenomenon. Two types of guided acoustic modes in the microscopically periodic and macroscopically inhomogeneous medium on the rigid bottom located at a depth $\bar{n}=\bar{n}_b$ for the case $\bar{n}_b>\bar{n}_c^{\min}$ of the incomplete screening of the caustic by the bottom. The dispersion relations $\bar{\Omega}_{L,H}=\bar{\Omega}_{L,H}(q_x)$ for the low-frequency (LF) and high-frequency (HF) modes are presented by the curves marked by $\bar{\Omega}_L$ and $\bar{\Omega}_H$, respectively. The positions of their undersurface channels in depth are grey in the insets of (b) and (d).

coordinate in HF acoustic mode than in LF acoustic mode. Recall that the physical meaning of the order p of the mode is the number of half-oscillations of the acoustic field at the width of a wave guide [28]. This analysis demonstrates that there are, in principle, two ways to get the same number p of vertical oscillations of the field across the gap-bottom channel—at lower frequencies in a wide channel, and at higher frequencies in a narrow channel located closer to the bottom than the first one.

Consequently, the existence of the rigid bottom could lead not just to a replacement of a single gap-caustic mode by two gap-bottom modes in the domains where $\bar{n}_c^{\mathrm{g/c}}>\bar{n}_b$ but could also introduce a gap-bottom mode additional to a gap-caustic mode in the domains where $\bar{n}_c^{\mathrm{g/c}}<\bar{n}_b$, without influencing on the gap-caustic mode. In other words, the existence of the rigid bottom, even below the gap-caustics channel, could modify the frequency spectrum of the wave-guide modes in the medium.

Potentially different situations arise in cases when $\bar{n}_b>\bar{n}_c^{\min}$ and there are intersections of $\bar{n}=\bar{n}_b$ with $\bar{n}=\bar{n}_c^{\mathrm{g/c}}$ [Figs. 5(b) and 5(d)] and in the case when $\bar{n}_b<\bar{n}_c^{\min}$ and the rigid boundary completely screens the caustic from the downwardly propagating rays [Figs. 6(b) and 6(d)]. The possible intersections of the bottom level $\bar{n}=\bar{n}_b$ with the gap level $\bar{n}=\bar{n}_g^{\mathrm{g/c}}$ of the gap-caustic modes in Figs. 5(b) and 5(d) play no role, because the positions of the gap for gap-bottom modes should be redefined. The generalized dispersion relation for the modes which are guided by the gap and either by the caustic or by the rigid boundary can be obtained by substituting $n_{\max}=\min[n_b,n_c]$ and $n_{\min}=n_g$ in Eq. (9).

Numerically evaluated characteristic cases are illustrated in Figs. 5 and 6. It can be seen that indeed two p modes, which we distinguish as high-frequency (HF) modes $\bar{\Omega}_H$ and low-frequency (LF) modes $\bar{\Omega}_L$, exist. For sufficiently long wavelengths ($q_x\ll 1$) these two modes are both guided between the gap and the bottom. If $\bar{n}_b>\bar{n}_c^{\min}$ then in both configurations when for $q_x=q_b^{\min}$, the bottom level where $\bar{n}=\bar{n}_b$ intersects the level $\bar{n}=\bar{n}_c^{\mathrm{g/c}}$ of the caustic for the gap-caustic mode, the gap-bottom channeling of the LF mode is transformed into its gap-caustic channeling [see Figs. 5(b) and 5(d)]. The gap-bottom channeling of the HF mode starts to coexist with gap-caustic channeling of the LF mode. In the $\oplus$ configuration this situation persists until a maximum allowed value of the propagation constant $q_x=1$ is reached, as shown in Fig. 5(b); on the other hand, in the $\otimes$ configuration, after the second intersection of $\bar{n}=\bar{n}_b$ with $\bar{n}=\bar{n}_c^{\mathrm{g/c}}$ at $q_x=q_b^{\max}$, the LF mode returns to channeling between the gap and the bottom as can be seen in Fig. 5(d). In summary the LF mode

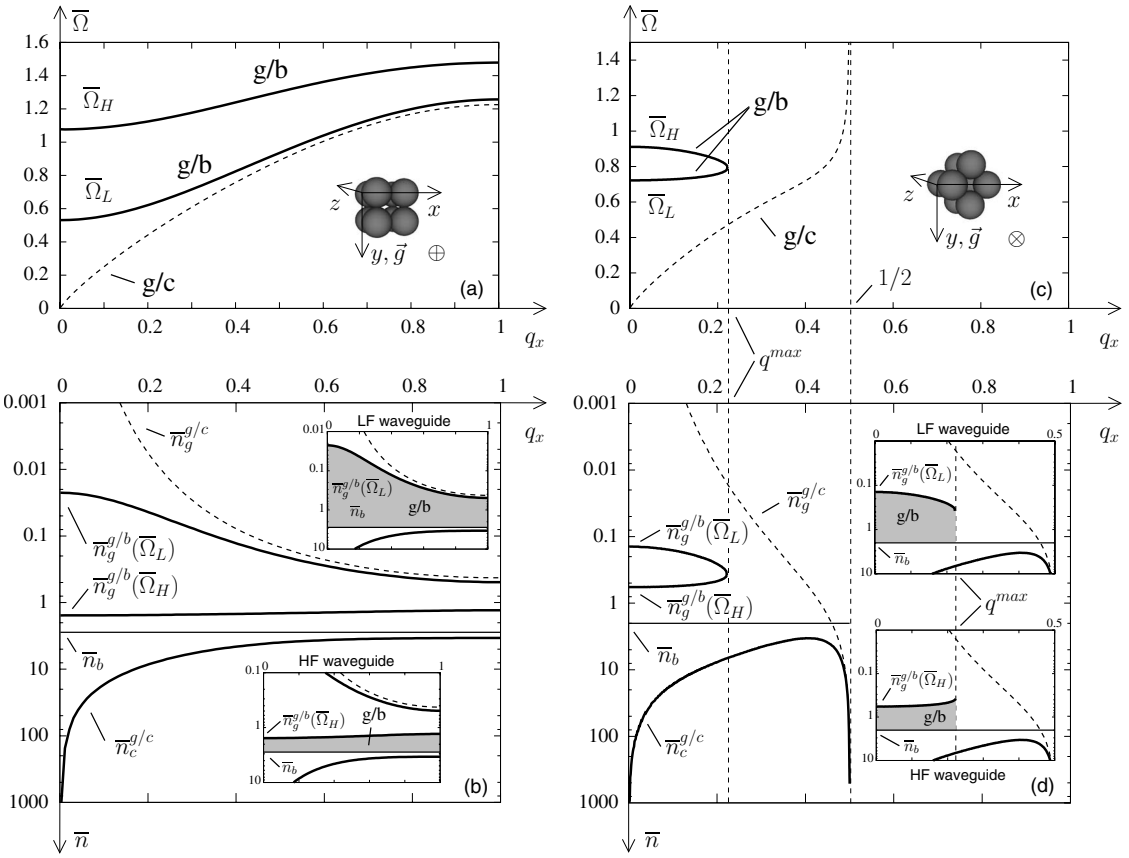

FIG. 6. Influence of a finite depth of granular medium on the wave-guiding phenomenon. Two types of guided acoustic modes in the microscopically periodic and macroscopically inhomogeneous medium on the rigid bottom located at a depth $\bar{n}=\bar{n}_b$ for the case $\bar{n}_b<\bar{n}_c^{\min}$ of the complete screening of the caustic by the bottom. The dispersion relations $\bar{\Omega}_{L,H}=\bar{\Omega}_{L,H}(q_x)$ for the low-frequency and high-frequency modes are presented by the curves marked by $\bar{\Omega}_L$ and $\bar{\Omega}_H$, respectively. The positions of their undersurface channels in depth are grey in the insets of (b) and (d).

travels between the gap at a depth $\bar{n}=\bar{n}_g^{\mathrm{g/b}}(\bar{\Omega}_L)$ marked by $\bar{n}=\bar{n}_g^{\mathrm{g/b}}(\bar{\Omega}_L)$ in Figs. 5(b) and 5(d) and either the bottom at a depth $\bar{n}=\bar{n}_b$ or the caustic at a depth $\bar{n}=\bar{n}_c^{\mathrm{g/c}}$, depending on which of these two surface is closer to the gap. When the gap-caustic (g/c) wave guiding of the LF mode is replaced by its gap-bottom (g/b) wave guiding [for $0\leqslant q_x\leqslant q_b^{\min}$ in the $\oplus$ configuration, Fig. 5(b), and for $0\leqslant q_x\leqslant q_b^{\min}$ and $q_b^{\min}\leqslant q_x\leqslant q_b^{\max}$ in the $\otimes$ configuration, Fig. 5(d)] the position of the upper boundary of the channel (the gap) is modified [compare dashed curves marked by $\bar{n}_g^{\mathrm{g/c}}$ and curves marked by $\bar{n}=\bar{n}_g^{\mathrm{g/b}}(\bar{\Omega}_L)$ in Figs. 5(b) and 5(d)]. The HF mode is an additional mode introduced by the presence of a rigid bottom. It always travels between the bottom at a depth $\bar{n}=\bar{n}_b$ and the gap at a depth $\bar{n}=\bar{n}_g^{\mathrm{g/b}}(\bar{\Omega}_H)$, marked by $\bar{n}_g^{\mathrm{g/b}}(\bar{\Omega}_H)$ in Figs. 5(b) and 5(d), even when the bottom is below the caustic at a depth $\bar{n}=\bar{n}_c^{\mathrm{g/c}}$. Two modes coexist for all $0\leqslant q_x\leqslant 1$ in the $\oplus$ configuration [Figs. 5(a) and 5(b)] and simultaneously disappear for $q_x>q_x^{\max}(q_x^{\max}\leqslant 1/2)$ in the $\otimes$ configuration [Figs. 5(c) and 5(d)].

When $\bar{n}_b<(\bar{n}_c^{\mathrm{g/c}})^{\min}$ (as shown in Fig. 6), the rigid bottom completely screens the caustic and only gap-bottom channeling can take place. Both LF and HF modes are traveling between the bottom at a depth $\bar{n}=\bar{n}_b$ and the gap, however, the positions of the gaps $\bar{n}=\bar{n}_g^{\mathrm{g/b}}(\bar{\Omega}_L)$ and $\bar{n}=\bar{n}_g^{\mathrm{g/b}}(\bar{\Omega}_H)$ [marked in Figs. 6(b) and 6(d) by $\bar{n}_g^{\mathrm{g/b}}(\bar{\Omega}_L)$ and $\bar{n}_g^{\mathrm{g/b}}(\bar{\Omega}_H)$, respectively] are different, and both are different from the position of the gap in gap-caustic wave-guiding configuration presented by dashed curves in Figs. 6(b) and 6(d). The HF mode travels in a narrower and deeper channel closer to the bottom than the LF mode. Two modes coexist for all $0\leqslant q_x\leqslant 1$ in the $\oplus$ configuration [Figs. 6(a) and 6(b)] and simultaneously disappear for $q_x>q_x^{\max}(q_x^{\max}\leqslant 1/2)$ in the $\otimes$ configuration [Figs. 6(c) and 6(d)].

This analysis shows how anisotropy influences the channeling of the LF and HF modes. While in the $\oplus$ configuration both the LF and HF modes coexist in the complete domain $0\leqslant q_x\leqslant 1$ of the propagation constants [see Figs. 5(a) and 5(b) and Figs. 6(a) and 6(b)] in the $\otimes$ configuration, on the other hand, the frequency gap between the modes shrinks progressively with increasing q_x until they simultaneously disappear at $q_x=q_x^{\max}\leqslant 1/2$. Wave guiding does not exist in the $\otimes$ configuration for the larger $(q_x>q_x^{\max})$ propagation constants.

CONCLUSIONS AND PERSPECTIVES

Although the details of the analytical theory have been developed only for the acoustic modes in unconsolidated or-

dered packing of spherical elastic grains under gravity, the wave-guide modes described here are universal in that they pertain to wave propagation in general—straightforward examples include electromagnetic propagation in inhomogeneous photonic crystals or acoustic wave motion in inhomogeneous composite materials. The theory confirmed through the analysis of the dispersion relations that natural subsurface channels for guiding of acoustic waves can exist due to the reflection of the acoustic waves at caustic and Bragg reflection by the granular lattice, the reflecting surfaces separated in space owing to the natural inhomogeneity of the phononic crystal. The positions of the subsurface gap-caustic channel for all allowed wave propagation constants, for the modes of different order p, and for different orientations of the granular crystal relative to the direction of gravitational acceleration have been predicted. The theory predicts that two types of guided modes can exist in the unconsolidated granular crystal layer on the rigid substrate, low-frequency and high-frequency modes of various order p can simultaneously propagate in partially overlapping under-surface channels. As well, the theory shows the influence of the saturation of medium inhomogeneity, adhesion between the grains, and the anisotropy of the granular crystals on the wave-guiding phenomenon.

The future development of the theory should address the analysis of the low order ($p \leqslant 3$) modes, because the geometrical acoustics approximation accepted by us here could be quantitatively imprecise in this limit. The theory could also be improved for cases where the gap is so close to the free surface of the granular crystal that the interaction of the channel with the surface through the evanescent acoustic field between them becomes important.

It is not difficult to envision wave-guiding phenomena in a wide variety of granular inhomogeneous materials ranging from ensembles of macroscopic elastic spheres constructed as efficient absorbers of sound and shock waves [31] or for a purpose of acoustic experiments [32] to nanotechnology, where the nanospheres are arranged in periodic arrays in sedimentation process [33–35]. The wave-guide acoustic modes of the types predicted here could be excited in the process of epitaxial growth of granular single crystals driven by vibrations [36,37] and of vibrational annealing of granular crystals [37,38]. Furthermore, the existence of these new wave guide modes suggest application of the monitoring of their propagation in unconsolidated granular phononic crystals to non-destructive analysis in a manner similar to how Rayleigh surface acoustic waves and Lamb wave-guide acoustic modes [28] are currently used in nondestructive testing and material evaluation [39].

ACKNOWLEDGMENT

This study has been supported by ANR Project No. NT05-341989.

[1] L. M. Brekhovskikh and O. A. Godin, *Acoustics of Layered Media I: Plane Waves and Quasi-Plane Waves* (Springer-Verlag, Berlin, 1990).
[2] O. A. Godin and D. M. F. Chapman, J. Acoust. Soc. Am. **106**, 2367 (1999).
[3] O. A. Godin and D. M. F. Chapman, J. Acoust. Soc. Am. **110**, 1890 (2001).
[4] P. H. Brownell, Science **197**, 497 (1977).
[5] P. H. Brownell, Sci. Am. **251**, 94 (1984).
[6] B. Andreotti, Phys. Rev. Lett. **93**, 238001 (2004).
[7] V. E. Gusev, V. Aleshin, and V. Tournat, Phys. Rev. Lett. **96**, 214301 (2006).
[8] V. Aleshin, V. Gusev, and V. Tournat, J. Acoust. Soc. Am. **121**, 2600 (2007).
[9] R. J. Urick, *Principles of Underwater Sound* (McGraw-Hill, New York, 1983).
[10] J. D. Joannopoulos, P. R. Villeneuve, and S. Fan, Nature (London) **386**, 143 (1997).
[11] S. Yang, J. H. Page, Z. Liu, M. L. Cowan, C. T. Chan, and P. Sheng, Phys. Rev. Lett. **88**, 104301 (2002).
[12] R. D. Mindlin and H. Deresiewicz, ASME Trans. J. Appl. Mech. **75**, 327 (1953).
[13] K. L. Johnson, *Contact Mechanics* (Cambridge University Press, Cambridge, 1985).
[14] M. Kafesaki, M. M. Sigalas, and N. Garcia, Phys. Rev. Lett. **85**, 4044 (2000).
[15] M. Wilm, A. Khelif, S. Ballandras, V. Laude, and B. Djafari-Rouhani, Phys. Rev. E **67**, 065602(R) (2003).
[16] A. Khelif, M. Wilm, V. Laude, S. Ballandras, and B. Djafari-Rouhani, Phys. Rev. E **69**, 067601 (2004).
[17] A. A. Maradudin, *Surface Phonons and Polaritons* (Garland STPM Press, New York, 1980).
[18] F. Gassmann, Geophysics **16**, 673 (1951).
[19] J. Duffy and R. D. Mindlin, ASME Trans. J. Appl. Mech. **24**, 585 (1957).
[20] R. D. Stroll, *Sediment Acoustics* (Springer-Verlag, Berlin, 1989).
[21] J. E. White, *Underground Sound* (Elsevier, Amsterdam, 1983).
[22] L. M. Schwartz, D. L. Johnson, and S. Feng, Phys. Rev. Lett. **52**, 831 (1984).
[23] A. N. Bogdanov and A. T. Skvortsov, Sov. Phys. Acoust. **38**, 224 (1992).
[24] Yu. A. Kravtsov and Yu. I. Orlov, *Geometrical Optics in Inhomogeneous Media* (Springer-Verlag, Berlin, 1989).
[25] E. Cosserat and F. Cosserat, *Theorie des Corps Deformables* (Hermann, Paris, 1909).
[26] V. I. Erofeev, Acoust. Phys. **40**, 223 (1994).
[27] L. D. Landau and E. M. Lifshitz, *Quantum Mechanics, Non-relativistic Theory, Vol. 3 of Course of Theoretical Physics* (Pergamon, New York, 1972).
[28] B. A. Auld, *Acoustic Fields and Waves in Solids* (Krieger, Malabar, 1990).
[29] P. G. De Gennes, Rev. Mod. Phys. **71**, S374 (1999).
[30] D. J. Hornbaker, R. Albert, I. Albert, A.-L. Barabási, and P. Schiffer, Nature (London) **387**, 765 (1997).
[31] V. F. Nesterenko, *Dynamics of Heterogeneous Materials*

(Springer, New York, 2001).
[32] D. L. Blair, N. W. Mueggenburg, A. H. Marshall, H. M. Jaeger, and S. R. Nagel, Phys. Rev. E **63**, 041304 (2001).
[33] Z. Cheng, W. B. Russel, and P. M. Chalkin, Nature (London) **401**, 893 (1999).
[34] J. D. Joannopoulos, Nature (London) **414**, 257 (2001).
[35] A. van Blaaden, R. Ruel, and P. Wiltzius, Nature (London) **385**, 321 (1997).
[36] Y. Nahmad-Molinari and J. C. Ruiz-Suarez, Phys. Rev. Lett. **89**, 264302 (2002).
[37] A. B. Yu, X. Z. An, R. P. Zou, R. Y. Yang, and K. Kendall, Phys. Rev. Lett. **97**, 265501 (2006).
[38] O. Carvente and J. C. Ruiz-Suarez, Phys. Rev. Lett. **95**, 018001 (2005).
[39] *Elastic Waves and Ultrasonic Nondestructive Evaluation*, edited by S. K. Datta, J. D. Achenbach, and Y. S. Rajapakse (Elsevier, Amsterdam, 1990).